

# Axion-photon Propagation in Magnetized Universe

Chen Wang<sup>a</sup> Dong Lai<sup>b</sup>

<sup>a</sup>National Astronomical Observatories, Chinese Academy of Sciences, A20 Datun Road, Chaoyang District, Beijing 100012, China

<sup>b</sup>Cornell Center for Astrophysics and Planetary Science, Department of Astronomy, Cornell University, Ithaca, NY 14853, USA

E-mail: [wangchen@nao.cas.cn](mailto:wangchen@nao.cas.cn), [dong@astro.cornell.edu](mailto:dong@astro.cornell.edu)

**Abstract.** Oscillations between photons and axion-like particles (ALP) travelling in intergalactic magnetic fields have been invoked to explain a number of astrophysical phenomena, or used to constrain ALP properties using observations. One example is the anomalous transparency of the universe to TeV gamma rays. The intergalactic magnetic field is usually modeled as patches of coherent domains, each with a uniform magnetic field, but the field orientation changes randomly from one domain to the next (“discrete- $\varphi$  model”). We show in this paper that in more realistic situations, when the magnetic field direction varies continuously along the propagation path, the photon-to-ALP conversion probability  $P$  can be significantly different from the discrete- $\varphi$  model. In particular,  $P$  has a distinct dependence on the photon energy and ALP mass, and can be as large as 100%. This result can affect previous constraints on ALP properties based on ALP-photon propagation in intergalactic magnetic fields, such as TeV photons from distant Active Galactic Nucleus.

**Keywords:** axion, gamma ray, magnetic field

**ArXiv ePrint:** [1511.03380](https://arxiv.org/abs/1511.03380)

---

## Contents

|          |   |           |
|----------|---|-----------|
| <b>1</b> | <b>Introduction.</b>                          | <b>1</b>  |
| <b>2</b> | <b>Equations</b>                              | <b>2</b>  |
| <b>3</b> | <b>Analytical Results</b>                     | <b>3</b>  |
| <b>4</b> | <b>Results for Random Magnetic Fields</b>     | <b>4</b>  |
| <b>5</b> | <b>Distribution of Conversion Probability</b> | <b>7</b>  |
| <b>6</b> | <b>Discussion</b>                             | <b>10</b> |

---

## 1 Introduction.

Axion is particle first introduced to solve the strong CP problem [1]. Axion-like particles (ALPs) also appear in many theoretically well-motivated extensions of the standard model of particle physics [2]. A general property of ALPs (represented by the field  $a$ ) is that they can couple to photons (represented by  $\mathbf{E}$ ) in the presence of an external magnetic field  $\mathbf{B}$  through the interaction Lagrangian  $\mathcal{L} = g a \mathbf{E} \cdot \mathbf{B}$ . While for axions there exists a relation between the coupling constant  $g$  and the axion mass  $m_a$ , in general  $g$  and  $m_a$  are unrelated for ALPs.

As a result of the photon-ALP coupling, a photon can oscillate into an ALP and vice versa in an external magnetic field. Such ALP-photon oscillations have been invoked to explain a variety of astrophysical phenomena, or conversely used to constrain the properties of ALPs using observations [3]. Examples include the apparent dimming of distant supernovae [4–6], spectral distortions of the cosmic microwave background [7, 8], and the dispersion of QSO spectra [6], et al. Recently, ALP-photon oscillation has been used to explain anomalous lack of opacity of the Universe to gamma rays: high energy gamma ray photons from Active Galactic Nuclei (AGNs) at cosmological distances have been detected by HESS, MAGIC and Fermi [9–13]. These photons can suffer significant attenuation before reaching Earth due to electron-positron pair production on the extragalactic background infrared radiation. Several analysis suggest that the Universe appears more transparent than expected based on recent extra-galactic background light models( [14–16]; however see [13, 17]). A possible explanation to the transparency problem is that because of the ALP-photon mixing, radiation from AGNs travels in the form of ALPs on a significant fraction of distance (without producing pairs) and converts back to photons before their detections [16, 18–26]. Another example concerns the possibilities that the recent observed 3.55keV photon line [27, 28] may arise from dark matter decay to ALPs and then convert to photons due to oscillations in the magnetic field of M31 and the Milky Way [29–33].

ALP-photon propagation over cosmological distance is strongly affected by the magnetic field structure. The primordial extragalactic magnetic field is most likely random and could described as patches of coherent domains with a typical magnitude upper limit of a few nG [34] and scale length of order a few Mpc [35]. Previous studies have adopted a simple model, in which the magnetic field is uniform in each domain, but the field orientation (characterized

by the angle  $\varphi$ ) changes in a random fashion from one domain to the next. Note that in this “discrete- $\varphi$ ” model, the photon-to-ALP conversion probability in each domain  $P_{\text{ad}}$  can be easily derived [see Eq. (3.4)] (since  $\varphi$  is constant in each domain). Assuming that  $\varphi$ ’s for different domains are random, Grossman et al. [36] then derived an expression for the photon-to-ALP conversion probability through a large number of domains [see Eq. (4.1)], and this expression has been widely used in many previous studies.

In realistic situations, the magnetic field and its orientation angle  $\varphi$  should vary continuously across neighboring domains. In fact, for a wide range of interesting ALP/magnetic field parameter space, the variation of  $\varphi$  with distance is sufficiently rapid that it cannot be neglected in almost all regions along the path of propagation. We show in this paper that a proper treatment of the random variation of the intergalactic magnetic field gives a qualitatively different result for the photon-to-ALP conversion probability compared to that obtained in the “discrete- $\varphi$ ” model.

For concreteness, we will focus on TeV photon-ALP propagating through intergalactic medium over cosmological distances, but our analysis and method can be easily re-scaled to other situations such as the Milky way or galaxy clusters, as well as for different photon energies.

## 2 Equations

The evolution equation of the photon electric field  $\mathbf{E}$  and ALP field  $a$  of a given angular frequency  $\omega$  or energy  $\mathcal{E}$  (so that  $\mathbf{E}, a \propto e^{i\omega t}$ ), expressed in a fixed Cartesian coordinates  $xyz$  (with the  $z$ -axis along the direction of propagation), takes the form

$$i \begin{pmatrix} a' \\ E'_x \\ E'_y \end{pmatrix} = \begin{pmatrix} \omega + \Delta_a & \Delta_M \cos \varphi & \Delta_M \sin \varphi \\ \Delta_M \cos \varphi & \omega + \Delta_{\text{pl}} & 0 \\ \Delta_M \sin \varphi & 0 & \omega + \Delta_{\text{pl}} \end{pmatrix} \begin{pmatrix} a \\ E_x \\ E_y \end{pmatrix}. \quad (2.1)$$

Here the superscript  $'$  stands for  $d/dz$ , and  $\varphi$  is the azimuthal angle of the magnetic field  $\mathbf{B}$  (more precisely,  $\varphi$  is the angle between  $\mathbf{B}_{\text{tr}}$ , the projection of  $\mathbf{B}$  in the  $xy$ -plane, and the  $x$ -axis). The ALP-mass-related parameter  $\Delta_a$  and the ALP-photon coupling parameter  $\Delta_M$  are given by

$$\Delta_a = -\frac{m_a^2}{2\omega} = -7.83 \times 10^{-2} \mathcal{E}_1^{-1} m_1^2 \text{ Mpc}^{-1}, \quad (2.2)$$

$$\Delta_M = \frac{1}{2} g B_{\text{tr}} = 4.63 \times 10^{-3} g_{11} B_1 \text{ Mpc}^{-1}, \quad (2.3)$$

where  $m_a$  is the ALP mass,  $\mathcal{E}$  is the photon energy,  $g$  is the axion-photon interaction parameter. We adopt units such that  $c = \hbar = 1$ , and define dimensionless quantities

$$\begin{aligned} m_1 &= m_a / (1 \text{ neV}), \\ \mathcal{E}_1 &= \mathcal{E} / (1 \text{ TeV}), \\ g_{11} &= g / (10^{-11} \text{ GeV}^{-1}), \\ B_1 &= B_{\text{tr}} / (1 \text{ nG}). \end{aligned} \quad (2.4)$$

The plasma parameter  $\Delta_{\text{pl}} = -\omega_{\text{pl}}^2 / (2\omega) = -1.11 \times 10^{-11} \mathcal{E}_1^{-1} (n_e / 10^{-7} \text{ cm}^{-3}) \text{ Mpc}^{-1}$  (where  $\omega_{\text{pl}}$  is the electron plasma frequency and  $n_e$  is the electron density) is unimportant for the parameter regime considered in this paper and will be neglected. Also, Eq. (2.1) does not include the QED effect, which is negligible for typical nG intergalactic magnetic fields [37]. All the numerical results presented in this paper are based on Eq. (2.1).

### 3 Analytical Results

For a given magnetic field structure, the ALP-photon evolution can be obtained by integrating Eq. (2.1) along the ray. Before studying complex random fields, we first consider two simple “single-domain” cases: (i)  $\varphi = 0$  independent of  $z$ ; (ii)  $\varphi$  increases linearly with  $z$ , with  $\varphi' = l^{-1}$ . Typical intergalactic magnetic fields have a coherence length of order  $l \sim 1$  Mpc, we define

$$l_1 = l/(1 \text{ Mpc}). \quad (3.1)$$

Note that, as a function of  $z/l$ , the photon-to-ALP conversion probability  $P$  depends only on the dimensionless quantities  $\Delta_a l$  and  $\Delta_M l$ , and thus on  $\mathcal{E}_1 m_1^{-2} l_1^{-1}$  and  $g_{11} B_1 l_1$ . Some numerical results are plotted in Fig. 1, showing that the photon-to-ALP conversion probabilities are quite different in the two cases.

To understand the difference analytically, we consider the evolution of  $E_{\parallel}$  and  $E_{\perp}$ , the components of  $\mathbf{E}$  parallel and perpendicular to  $\mathbf{B}_{\text{tr}}$ , respectively. Since  $E_{\parallel} = E_x \cos \varphi + E_y \sin \varphi$ ,  $E_{\perp} = -E_x \sin \varphi + E_y \cos \varphi$ , Eq. (2.1) can be rewritten as

$$i \begin{pmatrix} a' \\ E'_{\parallel} \\ E'_{\perp} \end{pmatrix} = \begin{pmatrix} \Delta_a & \Delta_M & 0 \\ \Delta_M & 0 & i\varphi' \\ 0 & -i\varphi' & 0 \end{pmatrix} \begin{pmatrix} a \\ E_{\parallel} \\ E_{\perp} \end{pmatrix}, \quad (3.2)$$

where we have dropped the non-essential term  $\omega$  in the diagonal elements.

If  $|\varphi'| \ll |\Delta_M|$ , Eq. (3.2) can be simplified to the evolution equation of  $a$  and  $E_{\parallel}$ :

$$i \begin{pmatrix} a' \\ E'_{\parallel} \end{pmatrix} \simeq \begin{pmatrix} \Delta_a & \Delta_M \\ \Delta_M & 0 \end{pmatrix} \begin{pmatrix} a \\ E_{\parallel} \end{pmatrix}. \quad (3.3)$$

This equation has been widely discussed in previous works. If the magnetic field strength varies slowly (we assume  $B_{\text{tr}}$  is constant along the ray for simplicity), the mode evolution is said to be “adiabatic”, and the photon-to-ALP conversion probability is given by the well-known formula [38]:

$$P_{\text{ad}} = \frac{\Delta_M^2}{(\Delta k/2)^2} \sin^2(\Delta k z/2), \quad (3.4)$$

with  $\Delta k = \sqrt{\Delta_a^2 + 4\Delta_M^2}$ . In the limit of  $\Delta k z/2 \ll 1$ , Eq. (3.4) simplifies to  $P_{\text{ad}} \simeq \Delta_M^2 z^2$ .

Intergalactic magnetic fields can often have  $|\varphi'| \sim 1 \text{ Mpc}^{-1}$ , much larger than  $|\Delta_a|$  and  $\Delta_M$  (see Eqs. 2-3). If  $|a| \ll |E|$ , the electric field can be solved as  $E_{\parallel} \simeq \cos \varphi$ ,  $E_{\perp} \simeq \sin \varphi$  assuming  $E_x = 1$ ,  $E_y = 0$  at  $z = 0$ , i.e.,  $\mathbf{E}(z) \simeq \mathbf{E}(z = 0)$ . Substitute this electric field into Eq. (3.2), we find the evolution equation for the ALP field,  $ia' \simeq \Delta_a a + \Delta_M \cos \varphi$ , with the solution

$$a(z) \simeq -e^{-i\Delta_a z} i \int_0^z dz \Delta_M \cos \varphi(z) e^{i\Delta_a z}. \quad (3.5)$$

For  $\varphi(z) = \varphi' z$  with constant  $\varphi'$ , we obtain the photon-to-ALP conversion probability

$$P = |a(z)|^2 \simeq \frac{\Delta_M^2}{\Delta_a^2 (1 - \varphi'^2/\Delta_a^2)^2} [(\cos \varphi - \cos \Delta_a z)^2 + (\varphi' \sin \varphi/\Delta_a - \sin \Delta_a z)^2]. \quad (3.6)$$

This equation accurately describes the numerical result of Fig. 1 for various values of  $\mathcal{E} m_a^{-2}$ . For example, in the limit of  $|\varphi'| \gg |\Delta_a|$ , Eq. (3.6) simplifies to  $P \simeq (\Delta_M/\varphi')^2 \sin^2 \varphi$ , which has an oscillation length  $\pi/\varphi'$  and is independent of the ALP mass and energy.

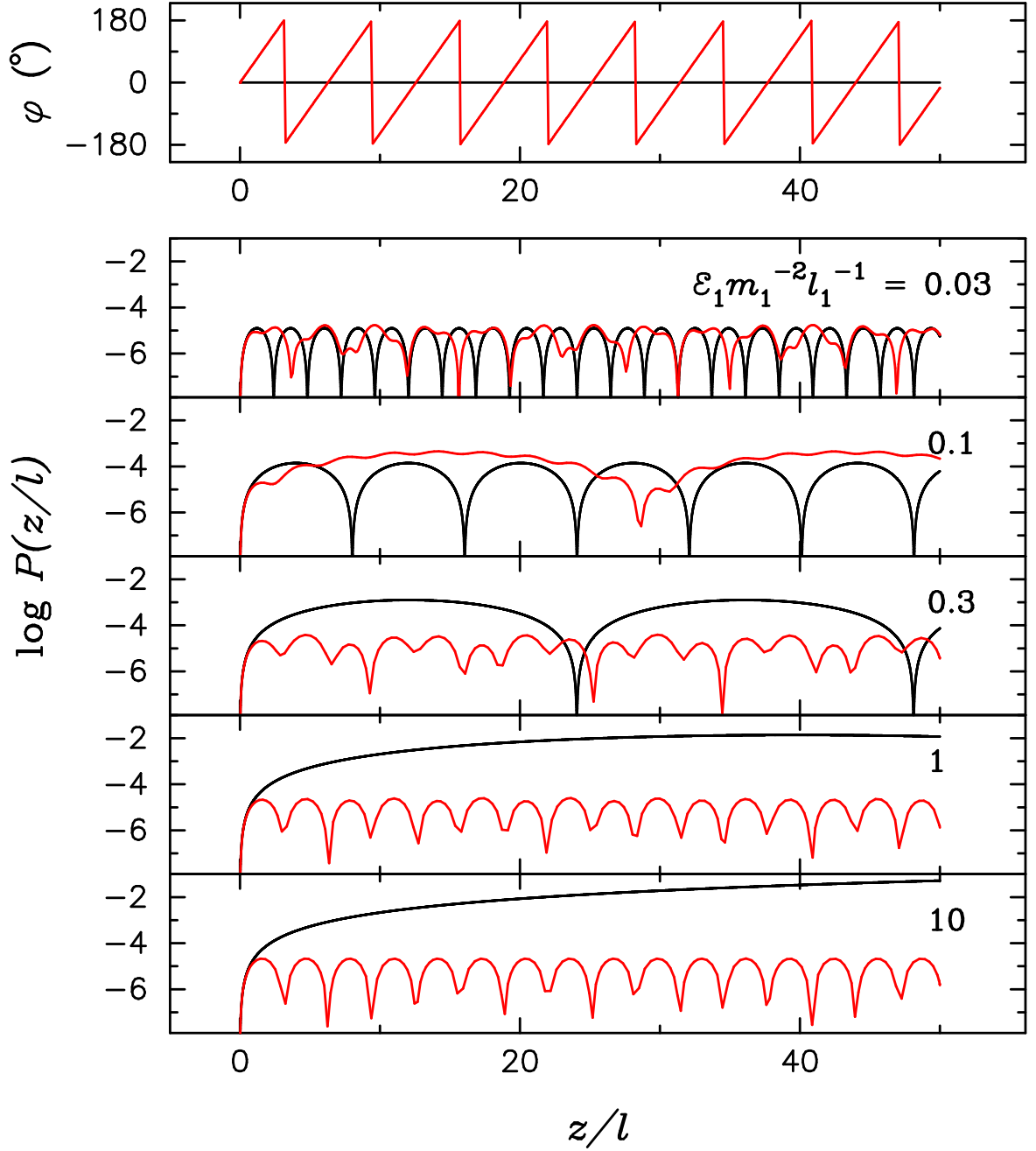


**Figure 1.** Photon-to-ALP conversion probability in single magnetic domain models for various values of  $\varepsilon_1 m_1^{-2} l_1^{-1}$ , all with  $g_{11} B_1 l_1 = 1$ . The black lines correspond to the model with  $\varphi = 0$  (constant field) in the whole domain along the ray, with  $P(z)$  analytically given by Eq. (3.4). The red lines correspond to the model with  $\varphi = l^{-1}z$ , with  $P(z)$  described by Eq. (3.6).

#### 4 Results for Random Magnetic Fields

The magnetic field in the intergalactic medium is randomly distributed, with the expected coherent length of order 0.1-1 Mpc (about the size of galaxy clusters). In general, numerical integrations are necessary to obtain the photon-to-axion conversion probability for a given realization of the random magnetic field distributions in addition to the relevant ALP

parameters. A “discrete- $\varphi$ ” model has been widely used in previous studies: The path of propagation is divided into many domains, each has the same size  $l$  and a uniform magnetic field, with the magnetic orientation angle  $\varphi$  changing randomly but discretely from one domain to the next. Based on this model, Ref. [36] derived an analytic expression for the mean value of the photo-to-ALP conversion probability after propagating through  $N$  domains (over distance  $z = Nl$ ):

$$P_{\text{ad},N} = \frac{1}{3} \left( 1 - e^{-3NP_{\text{ad}}/2} \right), \quad (4.1)$$

where on the right-hand side,  $P_{\text{ad}}$  is given by Eq. (3.4) evaluated at  $z = l$ . Note that for  $NP_{\text{ad}} \gg 1$ , we have  $P_{\text{ad},N} = 1/3$ , an upper limit for the conversion probability. In Fig. 2 we depict an example of the discrete- $\varphi$  model and the numerical results for the conversion probabilities at different values of  $\mathcal{E}m_a^{-2}$  (black lines). These numerical results are in agreement with Eq. (4.1) in the statistical sense.

As discussed above, we expect that the discrete- $\varphi$  model may be problematic since in most regions of the intergalactic medium  $|\varphi'|$  can be much larger than  $\Delta_M$ . In Fig. 2 (see the red lines) we consider a “linearly-continuous- $\varphi$ ” model: The path of propagation is again divided into many equal-sized domains; in each domain,  $\varphi$  varies linearly from one random value to another (thus,  $\varphi$  is always continuous,  $\varphi'$  is constant inside each domain but changes across the domain boundary). Our numerical results show that this continuous- $\varphi$  model can yield completely different conversion probabilities compared to the discrete- $\varphi$  model. In particular,  $P(z/l)$  exhibits quasi-periodicity along the ray (with the period dependent on  $\mathcal{E}m_a^{-2}l^{-1}$ ) and can be close to unity for large values of  $\mathcal{E}_1 m_1^{-2} l_1^{-1}$ .

To understand these numerical results, we apply Eq. (3.5) to the linearly-continuous- $\varphi$  model. The ALP amplitude after traversing  $N$  domains is given by

$$a_N \simeq -e^{-iN\Delta_a l} i \sum_{j=1}^N \Delta_M \int_{(j-1)l}^{jl} \cos \varphi(z) e^{i\Delta_a z} dz. \quad (4.2)$$

In the  $j$ -th domain,  $\varphi(z) = \varphi_{j-1} + \varphi'[z - (j-1)l]$ , with  $\varphi' = (\varphi_j - \varphi_{j-1})/l$ . For  $|\varphi'| \gg |\Delta_a|$  and  $|\Delta_a|l \ll 1$  (these two conditions are similar since  $|\varphi'| \sim l^{-1}$ ), Eq. (4.2) can be simplified, giving

$$|a_N|^2 \simeq \Delta_M^2 l^2 \left| \sum_{j=1}^N A_j(\varphi_j, \varphi_{j-1}) e^{ij\Delta_a l} \right|^2, \quad (4.3)$$

where

$$A_j \simeq \frac{\Delta\varphi(\sin \varphi_j - \sin \varphi_{j-1})}{\Delta\varphi^2 - \Delta_a^2 l^2} + \frac{i\Delta_a l(\cos \varphi_j - \cos \varphi_{j-1})}{\Delta\varphi^2 - \Delta_a^2 l^2}, \quad (4.4)$$

with  $\Delta\varphi = \varphi' l = \varphi_j - \varphi_{j-1}$ . For random  $\varphi_j$  (varying between  $-\pi$  and  $\pi$ ),  $A_j$  can be characterized by the mean  $\langle A \rangle$  and variance  $\sigma_A^2 = \langle |A_j - \langle A \rangle|^2 \rangle$ . The mean photo-to-ALP conversion probability  $P_N = \langle |a_N|^2 \rangle$  is then

$$P_N \simeq 0.123 \frac{\Delta_M^2}{\Delta_a^2} (1 - \cos N\Delta_a l) + \sigma_A^2 N \Delta_M^2 l^2, \quad (4.5)$$

where we have used  $|\langle A \rangle| \simeq \langle \frac{\sin \varphi_j - \sin \varphi_{j-1}}{\varphi_j - \varphi_{j-1}} \rangle \simeq 0.248$ . The variance  $\sigma_A^2$  can be calculated using Monte-Carlo method, and we find  $\sigma_A^2 \simeq 0.44, 0.30$  and  $0.23$  for  $\mathcal{E}_1 m_1^{-2} l_1^{-1} = 0.3, 1$  and  $\gtrsim 10$

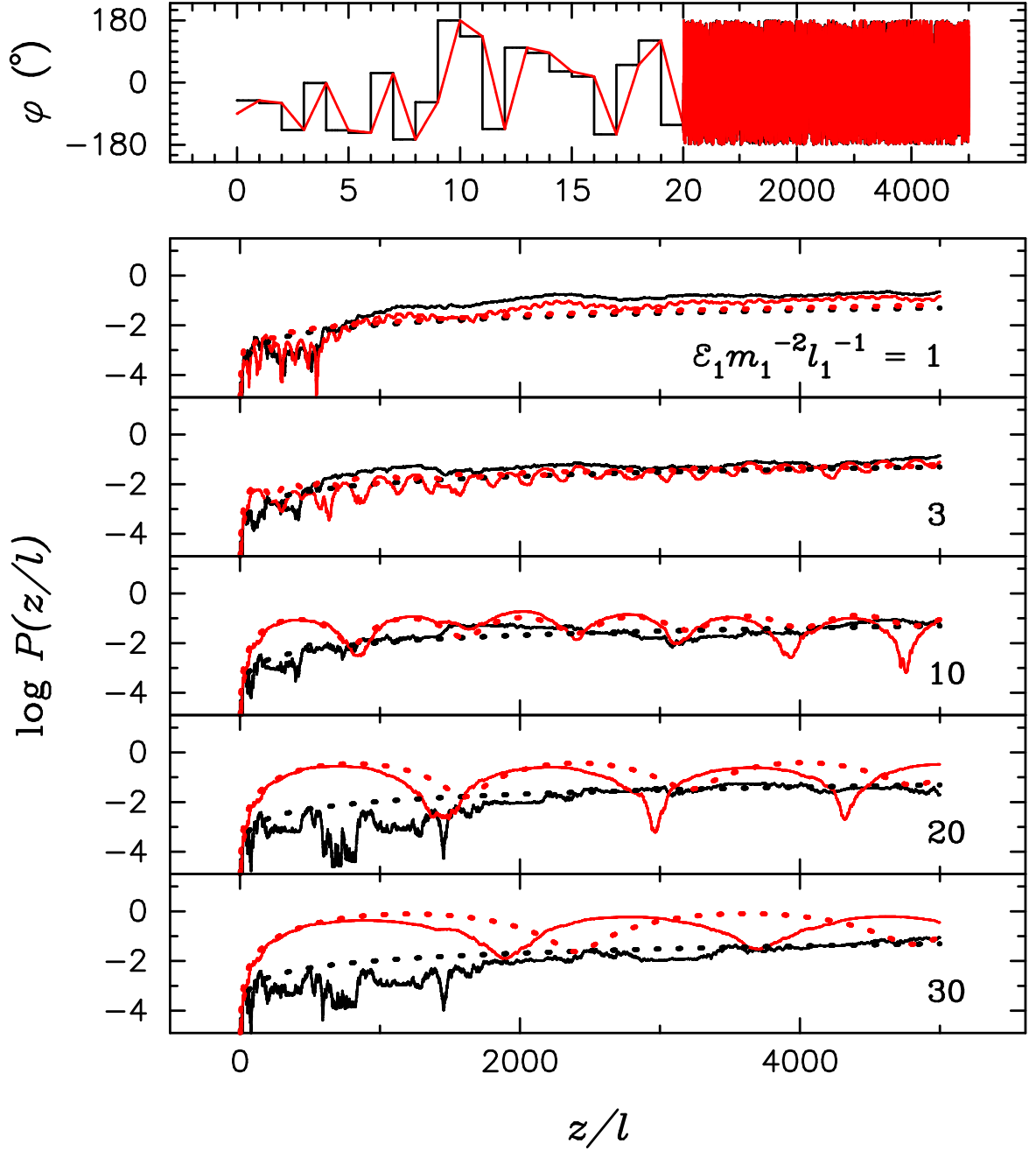


**Figure 2.** Photon-to-ALP conversion probability across multiple domains of the intergalactic medium with random magnetic fields. Each domain has the same size  $l$  and magnetic field strength. The top panel depicts an example of the magnetic orientation angle in two different models: The black line for the discrete- $\varphi$  model and the red line for the linearly-continuous- $\varphi$  model. The lower panels show the numerical results for the conversion probability for various values of  $\varepsilon m_a^{-2} l^{-1}$  (all with  $B_1 g_{11} l_1 = 1$ ), for the discrete- $\varphi$  model (black lines) and the linearly-continuous- $\varphi$  model (red lines). The black-dotted and red-dotted lines correspond to the analytical expressions (4.1) and (4.5), respectively.

(corresponding to  $|\Delta_a|l = 0.26, 0.078$  and  $\lesssim 0.0078$ ). Note that the validity of Eq. (4.5) requires  $|\Delta_a|l \ll 1$ ,  $\Delta_M l \ll 1$  and  $|a| \ll |\mathbf{E}|$  (or  $P_N \ll 1$ ). Under the same condition, Eq. (4.1) reduces to  $P_{\text{ad},N} \simeq 0.5 N \Delta_M^2 l^2$ , similar to the second term in Eq. (4.5).

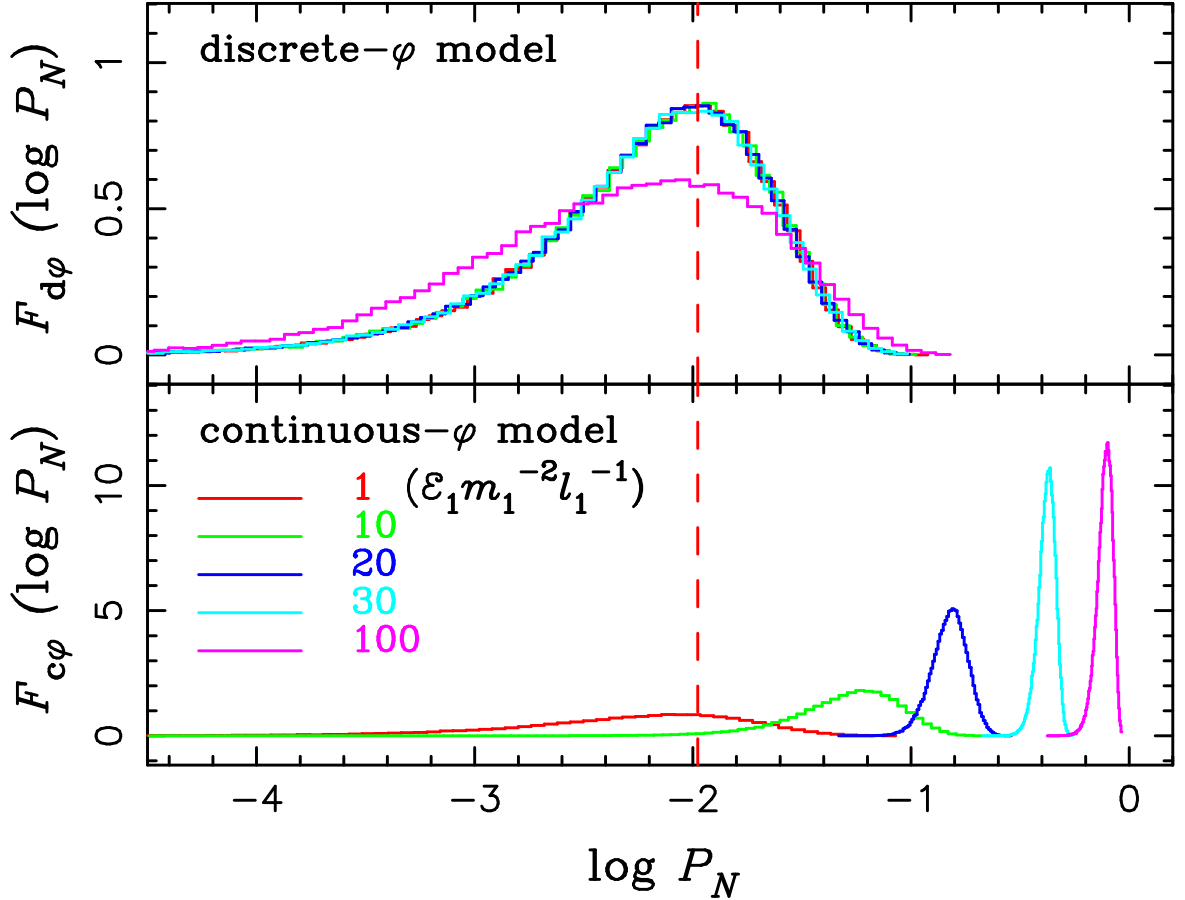


**Figure 3.** The distribution function of the photon-to-ALP conversion probability after a distance of 1 Gpc. The upper and lower panels correspond to the discrete- $\varphi$  model and the linearly-continuous- $\varphi$  model, respectively (see Fig. 2). The different curves are for different values of  $\mathcal{E}_1 m_1^{-2} l_1^{-1}$ , all with  $g_{11} B_1 l_1^{-1} = 1$ , the domain size  $l = 1$  Mpc and the domain number  $N = 1000$ . The vertical red dashed line represents the theoretical conversion probability of the discrete- $\varphi$  model, given by Eq. (4.1).

Equation (4.5) indicates that the photon-to-ALP conversion probability has a cosine function dependence, with the oscillation length (in units of  $l$ )  $2\pi/|\Delta_a l| \simeq 80 \mathcal{E}_1 m_1^{-2} l_1^{-1}$ . This is in agreement with numerical results presented in Fig. 2, especially for  $1 \lesssim \mathcal{E}_1 m_1^{-2} l_1^{-1} \lesssim 30$ . For  $\mathcal{E}_1 m_1^{-2} l_1^{-1} \lesssim 1$ , the inequality  $|\Delta_a| \ll |\varphi'|$  is not well satisfied; for  $\mathcal{E}_1 m_1^{-2} l_1^{-1} \gtrsim 30$ , the ALP amplitude can be comparable to  $|\mathbf{E}|$ , making Eq. (4.5) inaccurate.

## 5 Distribution of Conversion Probability

Because the intergalactic magnetic field has random orientations along the propagation path, the conversion probability  $P_N$  has a distribution with finite spread. To obtain the  $P_N$  distribution, we carry out Monte-Carlo calculations of the photon-ALP propagations for  $10^5$  times, each time with the same set of ALP and magnetic field parameters, but for different random values of  $\varphi$  in each domain. We consider both the discrete  $\varphi$  model and the linearly-continuous  $\varphi$  model as discussed above. The results are shown in Fig. 3.

For the discrete- $\varphi$  model, the  $P_N$ -distribution function,  $F_{d\varphi}(\log P_N)$ , is a skewed Gaussian (see the upper panel of Fig. 3). The peak of the distribution is accurately predicted



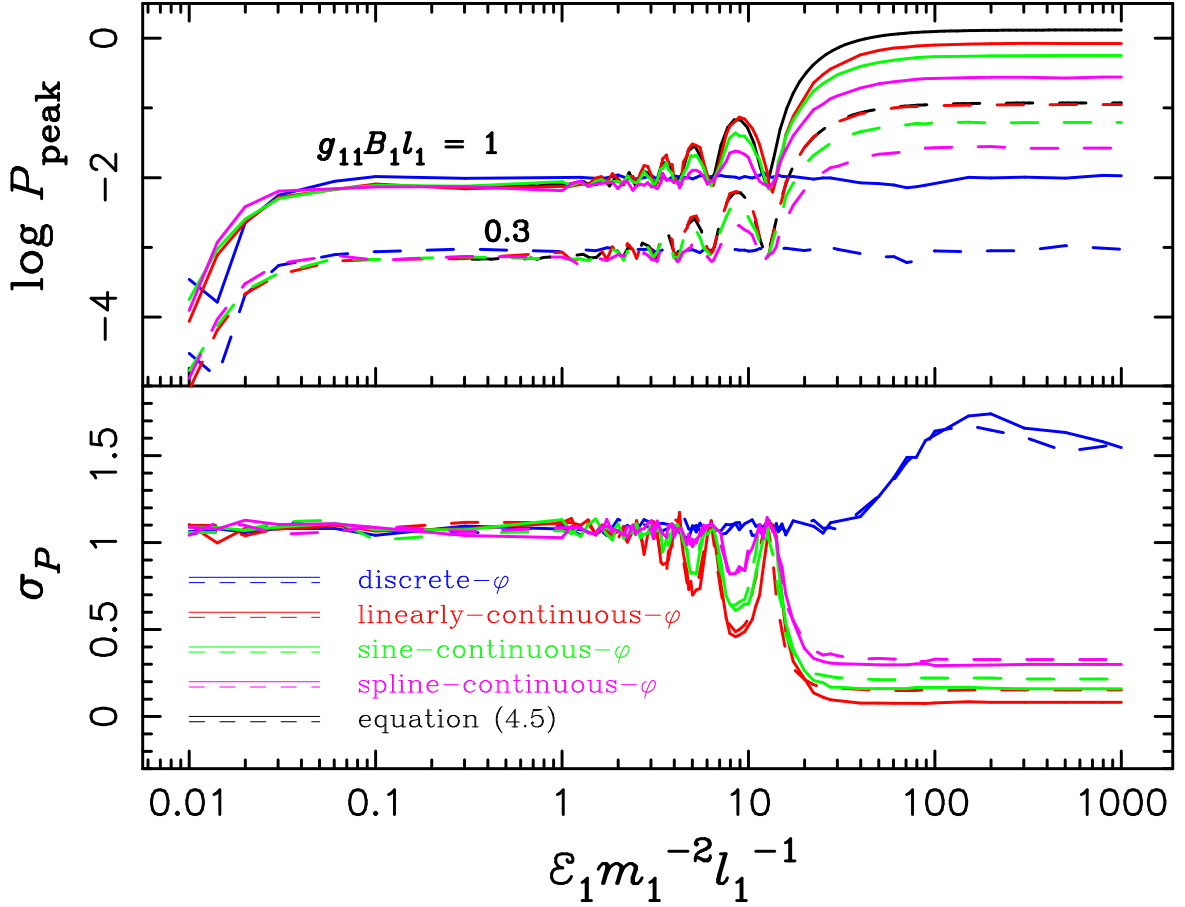
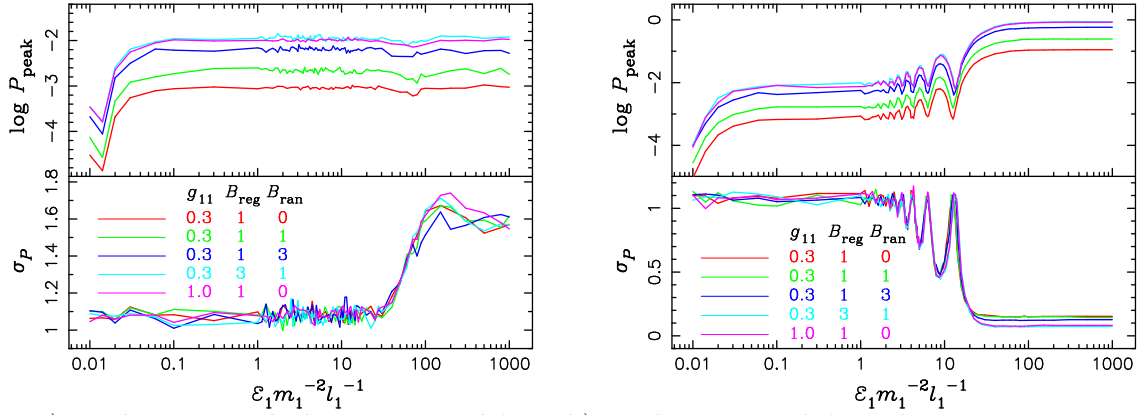


**Figure 4.** Peak position  $P_{\text{peak}}$  and half-peak width  $\sigma_P$  of the  $P_N$ -distribution function across  $\mathcal{E}m_a^{-2}l^{-1}$ . Two different values of  $g_{11}B_1l_1$  ( $= 0.3, 1$ ) are presented as dashed and solid lines. Lines with different colors correspond to different  $\varphi$  models (as indicated in the lower panel). The black lines in the upper panel show the analytical equation (4.5). The other parameters are the same as in Fig. 3.

by Eq. (4.1). We find that  $F_{d\varphi}(\log P_N)$  is almost the same for different values of  $\mathcal{E}m_a^{-2}l^{-1}$ , except that for  $\mathcal{E}_1m_1^{-2}l_1^{-1} \gtrsim 40$  the distribution becomes a broader.

The lower panel of Fig. 3 shows the  $P_N$ -distribution function  $F_{c\varphi}(\log P_N)$  for the linearly-continuous  $\varphi$  model. For  $\mathcal{E}_1m_1^{-2}l_1^{-1} \lesssim 1$  the distribution function is similar to that of the discrete- $\phi$  model. However, as  $\mathcal{E}_1m_1^{-2}l_1^{-1}$  increases, the peak of the distribution shifts to larger values and the width becomes narrower – these features are in marked contrast to the discrete- $\varphi$  model.

To characterize how the  $P_N$ -distribution function varies for different parameters, we show in Fig. 4  $P_{\text{peak}}$  and  $\sigma_P$ , the peak and half-peak width of the distribution for two different values of  $g_{11}B_1l_1$ , as a function of  $\mathcal{E}_1m_1^{-2}l_1^{-1}$  (the other parameters are the same as in Fig. 3). For the discrete- $\varphi$  model (blue lines in Fig. 4),  $P_{\text{peak}}$  is almost independent of  $\mathcal{E}_1m_1^{-2}l_1^{-1}$ , except when the oscillation length is smaller than domain size, i.e., when  $\Delta kl/2 \gtrsim 1$  or  $\mathcal{E}_1m_1^{-2}l_1^{-1} \lesssim 0.04$ . The value of  $P_{\text{peak}}$  can be accurately predicted by Eq. (4.1). The width of the distribution is almost constant except for  $\mathcal{E}_1m_1^{-2}l_1^{-1} \gtrsim 40$ . Note that for  $g_{11}B_1l_1 \gtrsim 10$ , the conversion probability is close to the upper limit  $1/3$ , and the  $P_N$  distribution is not a Gaussian.



a) random  $B_{\text{tr}}$  with discrete- $\varphi$  model      b) random  $B_{\text{tr}}$  with linearly-continuous- $\varphi$  model

**Figure 5.** Similar to Fig. 4, except that the magnetic field magnitudes  $B_{\text{tr}}$  in different domains are different and are randomly distributed in the range of  $B_{\text{reg}}$  and  $B_{\text{reg}} + B_{\text{ran}}$ . The Colored lines correspond to different values of  $g_{11}$ ,  $B_{\text{reg}}$  and  $B_{\text{ran}}$  as indicated (the units of  $B$  is nG). Panel a) and b) represent the discrete- $\varphi$  and linearly-continuous- $\varphi$  models, respectively. The other parameters are the same as in Fig. 3.

For the linearly-continuous  $\varphi$  model (red lines in Fig. 4), larger  $\mathcal{E}_1 m_1^{-2} l_1^{-1}$  generally leads to larger  $P_{\text{peak}}$  and smaller  $\sigma_P$ . Interestingly, both  $P_{\text{peak}}$  and  $\sigma_P$  are not a monotonous function of  $\mathcal{E}_1 m_1^{-2} l_1^{-1}$ , but have oscillations. This oscillation can be described by Eq. (4.5), as shown by the black lines in Fig. 4 [Note that Eq. (4.5) is valid only for  $|\Delta_a| l \ll 1$ , so we choose the dotted lines start from  $\mathcal{E}_1 m_1^{-2} l_1^{-1} \simeq 0.3$ ]. For  $\mathcal{E}_1 m_1^{-2} l_1^{-1} \lesssim 1$ , both  $P_{\text{peak}}$  and  $\sigma_P$  are almost the same as in the discrete- $\varphi$  model. In the case of  $g_{11} B_1 l_1 = 0.3$  (blue lines), Eq. (4.5) agrees very well with the numerical result, since the assumption  $|a| \ll |\mathbf{E}|$  always tenable. For  $|N \Delta_a l| \ll 1$  [or  $\mathcal{E}_1 m_1^{-2} l_1^{-1} \gg 78 N / 10^3$ ], the conversion probability reaches its maximum  $P_{\text{max}} \simeq 0.0615 N^2 \Delta_M^2 l^2 = 1.3 (g_{11} B_1 l_1)^2 (N / 10^3)^2$ . In the case of  $g_{11} B_1 l_1 = 1$ , the peak conversion probability  $P_{\text{peak}}$  approaches unity for  $\mathcal{E}_1 m_1^{-2} l_1^{-1} \gtrsim 40$ , implying a nearly 100% photon-to-ALP conversion [Of course, the analytical expression (4.5) is less accurate when  $P_{\text{peak}} \sim 1$  since  $|a| \ll |\mathbf{E}|$  is invalid].

In the above, we have focused on the linearly-continuous- $\varphi$  model, since in this case we can derive analytical equations [see Eqs. (3.6) and (4.5)] to help understand our numerical results. We have performed calculations for other continuous- $\varphi$  models, e.g., using the spline function or sine function to link the random  $\varphi$  values in multiple domains (see Fig. 4). We find that the results for the  $P_N$  distribution are similar to the linearly-continuous- $\varphi$  model, although the conversion probabilities are slightly lower because in the spline and sine  $\varphi$  models there always exist some regions with  $\varphi' \sim 0$ .

So far in this paper we have assumed that the magnetic field has the same strength  $B_{\text{tr}}$  in different domains but with varying orientations. What happens when  $B_{\text{tr}}$  also varies? For concreteness, we consider a simple model where the values of  $B_{\text{tr}}$  in different domains are randomly distributed in the range between  $B_{\text{reg}}$  and  $B_{\text{reg}} + B_{\text{ran}}$ . Our numerical results for the final  $P_N$  distributions (for both discrete- $\varphi$  and continuous- $\varphi$  models) for various values of  $g$ ,  $B_{\text{reg}}$  and  $B_{\text{ran}}$  are shown in Figure 5. The results are very similar to the constant  $B_{\text{tr}}$  case shown in Fig. 4. For the discrete- $\varphi$  model (Fig. 5a), we can derive an analytical expression of the final conversion probability using Eq. (4.2) (with  $\varphi(z) = \text{constant}$  in each domain, but

$\Delta_M$  and  $\varphi$  have different values in different domains). For  $|\Delta_a|l \ll 1$ , we find

$$P_{\text{ranB},N} = N \langle \Delta_M^2 l^2 \cos^2 \varphi_j \rangle = \frac{1}{8} N g^2 l^2 \langle B_{\text{tr}}^2 \rangle, \quad (5.1)$$

where  $\langle B_{\text{tr}}^2 \rangle = B_{\text{reg}}^2 + B_{\text{reg}} B_{\text{ran}} + B_{\text{ran}}^2/3$ . The above equation is the same as the case with constant  $B_{\text{tr}}$  and discrete  $\varphi$  ( $P_{\text{ad},N} = 0.5 N \Delta_M^2 l^2$ ), if we replace  $B_{\text{tr}}$  by  $\sqrt{\langle B_{\text{tr}}^2 \rangle} = \sqrt{B_{\text{reg}}^2 + B_{\text{reg}} B_{\text{ran}} + B_{\text{ran}}^2/3}$ . Equation (5.1) agrees well with the numerical results shown in Fig. 5a. The same applies for the linearly-continuous- $\varphi$  model: the  $P_{\text{peak}}$  curves shown in Fig. 5b are almost the same as the constant  $B_{\text{tr}}$  case if we replace  $B_{\text{tr}}$  by  $\sqrt{\langle B_{\text{tr}}^2 \rangle}$ .

## 6 Discussion

We have shown that a proper treatment of the inhomogeneity of intergalactic magnetic fields can lead to very different photon-to-ALP conversion probabilities compared to the “discrete- $\varphi$ ” model widely used in previous studies. The difference is particularly striking when  $\mathcal{E}_1 m_1^{-2} l_1^{-1} \gtrsim 4\sqrt{N/10^3}$  [the first term of Eq. (4.5) larger than the second term; here  $l$  is the coherence length of the magnetic field domain and  $N = z/l$  the domain numbers across distance  $z$ ]. In the discrete- $\varphi$  model, the conversion probability is determined by  $\Delta_M l \propto gBl$  and almost does not depend on  $\Delta_a l$  or  $\mathcal{E} m_a^{-2} l^{-1}$  (assuming  $|\Delta_a|l \ll 1$  and  $\Delta_M l \ll 1$ ), and never exceeds 1/3 [see Eq. (4.1)]. By contrast, in the continuous- $\varphi$  model, the photon-to-axion conversion probability has a distinct dependence on  $\mathcal{E}_1 m_1^{-2} l_1^{-1}$ ; it becomes significant when  $|\Delta_a| \lesssim \Delta_M$  [see Eqs. (2)-(3)] and can be as large as 100% (see Figs. 3-4). Our analytic expression (4.5) (valid for  $|\Delta_a|l \ll 1$ ,  $\Delta_M l \ll 1$  and  $P_N \lesssim 1$ ) approximately captures these features.

Note that although we have considered TeV photon-ALP propagation in intergalactic magnetic fields (with  $B_{\text{tr}} \sim 1$  nG,  $l \sim 1$  Mpc), our results can be easily re-scaled to different situations. For example, Ref. [22] explored the hardening of the TeV photon spectrum of Blazars due to the  $\gamma \rightarrow a \rightarrow \gamma$  conversions in the magnetic fields of galaxy clusters and Milky Way. In galaxy clusters,  $B_{\text{tr}} \sim 1$   $\mu$ G,  $l \sim 10$  kpc, we have

$$\begin{aligned} \mathcal{E}_1 m_1^{-2} l_1^{-1} &= \frac{\mathcal{E}}{1 \text{ TeV}} \left( \frac{m_a}{10^{-8} \text{ eV}} \right)^{-2} \left( \frac{l}{10 \text{ kpc}} \right)^{-1}, \\ g_{11} B_1 l_1 &= \frac{g}{10^{-12} \text{ GeV}} \frac{B_{\text{tr}}}{1 \mu\text{G}} \frac{l}{10 \text{ kpc}}. \end{aligned} \quad (6.1)$$

Thus with  $m_a \sim 10^{-8}$  eV,  $g \sim 10^{-12}$  GeV (see [22]), the conversion of TeV photon-to-ALP in the galaxy clusters can be significantly affected by our results. ALPs can convert back to be TeV photons in the magnetic field of the Milky Way. Similar ALP-to-photon conversion in M31 and the Milky Way are used to explain the recent observations of the 3.55 keV photon line [29–33]. Our results can be easily adapted to the typical galactic magnetic field ( $B_{\text{tr}} \sim 10$   $\mu$ G,  $l \sim 100$  pc–1 kpc) with different  $\mathcal{E}$ ,  $g$  and  $m_a$ .

In summary, many previous works use the discrete- $\varphi$  model and Eq. (4.1) to estimate the photon-to-ALP conversion probabilities. In light of the significant difference between the discrete and continuous- $\varphi$  models of magnetic fields, a re-evaluation of the previous results is warranted.

## Acknowledgements

This work has been supported in part by the National Natural Science Foundation of China (11273029), and by NSF grant AST-1211061 and NASA grant NNX14AG94G.

## References

- [1] R. D. Peccei and Helen R. Quinn. C<sub>p</sub> conservation in the presence of pseudoparticles. *Physical Review Letters*, 38:1440–1443, 1977.
- [2] Joerg Jaeckel and Andreas Ringwald. The low-energy frontier of particle physics. *Annual Review of Nuclear and Particle Science*, 60:405–437, 2010.
- [3] Alessandro Mirizzi, Georg G. Raffelt<sup>1</sup>, Pasquale D. Serpico, Georg Raffelt, and Berta Beltrn. Photon-axion conversion in intergalactic magnetic fields and cosmological consequences, n/a 1, 2008 2008.
- [4] Csaba Cski, Nemanja Kaloper, and John Terning. Dimming supernovae without cosmic acceleration. *Physical Review Letters*, 88:161302, 2002.
- [5] Alessandro Mirizzi, Georg G. Raffelt, and Pasquale D. Serpico. Photon-axion conversion as a mechanism for supernova dimming: Limits from cmb spectral distortion. *Physical Review D*, 72:23501, 2005.
- [6] Linda stman and Edvard Mrtzell. Limiting the dimming of distant type ia supernovae. *Journal of Cosmology and Astro-Particle Physics*, 02:005, 2005.
- [7] A. G. Dias, A. C. B. Machado, C. C. Nishi, A. Ringwald, and P. Vaudrevange. The quest for an intermediate-scale accidental axion and further alps. *Journal of High Energy Physics*, 06, 2014.
- [8] Csaba Csaki, Nemanja Kaloper, and John Terning. Planck data and ultralight axions, May 1, 2014 2014. 15 pages, 4 figures.
- [9] F. Aharonian, A. G. Akhperjanian, A. R. Bazer-Bachi, M. Beilicke, W. Benbow, D. Berge, K. Bernlhr, C. Boisson, O. Bolz, V. Borrel, I. Braun, F. Breitling, A. M. Brown, P. M. Chadwick, L.-M. Chounet, R. Cornils, L. Costamante, B. Degrange, H. J. Dickinson, A. Djannati-Ata, L. O’c. Drury, G. Dubus, D. Emmanoulopoulos, P. Espigat, F. Feinstein, G. Fontaine, Y. Fuchs, S. Funk, Y. A. Gallant, B. Giebels, S. Gillessen, J. F. Glicenstein, P. Goret, C. Hadjichristidis, D. Hauser, M. Hauser, G. Heinzelmann, G. Henri, G. Hermann, J. A. Hinton, W. Hofmann, M. Holleran, D. Horns, A. Jacholkowska, O. C. de Jager, B. Khelifi, S. Klages, Nu. Komin, A. Konopelko, I. J. Latham, R. Le Gallou, A. Lemiore, M. Lemoine-Goumard, N. Leroy, T. Lohse, J. M. Martin, O. Martineau-Huynh, A. Marcowith, C. Masterson, T. J. L. McComb, M. de Naurois, S. J. Nolan, A. Noutsos, K. J. Orford, J. L. Osborne, M. Ouchrif, M. Panter, G. Pelletier, S. Pita, G. Phlhofer, M. Punch, B. C. Raubenheimer, M. Raue, J. Raux, S. M. Rayner, A. Reimer, O. Reimer, J. Ripken, L. Rob, L. Rolland, G. Rowell, V. Sahakian, L. Saug, S. Schlenker, R. Schlickeiser, C. Schuster, U. Schwanke, M. Siewert, H. Sol, D. Spangler, R. Steenkamp, C. Stegmann, J.-P. Tavernet, R. Terrier, C. G. Thoret, M. Tluczykont, C. van Eldik, G. Vasileiadis, C. Venter, P. Vincent, et al. A low level of extragalactic background light as revealed by -rays from blazars. *Nature*, 440:1018–1021, 2006.
- [10] D. Mazin and M. Raue. New limits on the density of the extragalactic background light in the optical to the far infrared from the spectra of all known tev blazars. *Astronomy and Astrophysics*, 471:439–452, 2007.
- [11] MAGIC Collaboration, J. Albert, E. Aliu, H. Anderhub, L. A. Antonelli, P. Antoranz, M. Backes, C. Baixeras, J. A. Barrio, H. Bartko, D. Bastieri, J. K. Becker, W. Bednarek, K. Berger, E. Bernardini, C. Bigongiari, A. Biland, R. K. Bock, G. Bonnoli, P. Bordas, V. Bosch-Ramon, T. Bretz, I. Britvitch, M. Camara, E. Carmona, A. Chilingarian, S. Commichau, J. L. Contreras, J. Cortina, M. T. Costado, S. Covino, V. Curtef, F. Dazzi,

- A. De Angelis, E. De Cea del Pozo, R. de los Reyes, B. De Lotto, M. De Maria, F. De Sabata, C. Delgado Mendez, A. Dominguez, D. Dorner, M. Doro, M. Errando, M. Fagiolini, D. Ferenc, E. Fernandez, R. Firpo, M. V. Fonseca, L. Font, N. Galante, R. J. Garca Lpez, M. Garczarczyk, M. Gaug, F. Goebel, M. Hayashida, A. Herrero, D. Hhne, J. Hose, C. C. Hsu, S. Huber, T. Jogler, T. M. Kneiske, D. Kranich, A. La Barbera, A. Laille, E. Leonardo, E. Lindfors, S. Lombardi, F. Longo, M. Lpez, E. Lorenz, P. Majumdar, G. Maneva, N. Mankuzhiyil, K. Mannheim, L. Maraschi, M. Mariotti, M. Martnez, D. Mazin, M. Meucci, M. Meyer, J. M. Miranda, R. Mirzoyan, S. Mizobuchi, M. Moles, A. Moralejo, D. Nieto, K. Nilsson, J. Ninkovic, N. Otte, I. Oya, M. Panniello, R. Paoletti, J. M. Paredes, M. Pasanen, D. Pascoli, F. Pauss, R. G. Pegna, M. A. Perez-Torres, et al. Very-high-energy gamma rays from a distant quasar: How transparent is the universe? *Science*, 320:1752–, 2008.
- [12] M. Ackermann, M. Ajello, A. Allafort, P. Schady, L. Baldini, J. Ballet, G. Barbiellini, D. Bastieri, R. Bellazzini, R. D. Blandford, E. D. Bloom, A. W. Borgland, E. Bottacini, A. Bouvier, J. Bregeon, M. Brigida, P. Bruel, R. Buehler, S. Buson, G. A. Caliendo, R. A. Cameron, P. A. Caraveo, E. Cavazzuti, C. Cecchi, E. Charles, R. C. G. Chaves, A. Chekhtman, C. C. Cheung, J. Chiang, G. Chiaro, S. Ciprini, R. Claus, J. Cohen-Tanugi, J. Conrad, S. Cutini, F. D’Ammando, F. de Palma, C. D. Dermer, S. W. Digel, E. do Couto e Silva, A. Domnguez, P. S. Drell, A. Drlica-Wagner, C. Favuzzi, S. J. Fegan, W. B. Focke, A. Franckowiak, Y. Fukazawa, S. Funk, P. Fusco, F. Gargano, D. Gasparrini, N. Gehrels, S. Germani, N. Giglietto, F. Giordano, M. Giroletti, T. Glanzman, G. Godfrey, I. A. Grenier, J. E. Grove, S. Guiriec, M. Gustafsson, D. Hadasch, M. Hayashida, E. Hays, M. S. Jackson, T. Jogler, J. Kataoka, J. Knudsen, M. Kuss, J. Lande, S. Larsson, L. Latronico, F. Longo, F. Loparco, M. N. Lovellette, P. Lubrano, M. N. Mazziotta, J. E. McEnery, J. Mehault, P. F. Michelson, T. Mizuno, C. Monte, M. E. Monzani, A. Morselli, I. V. Moskalenko, S. Murgia, A. Tramacere, E. Nuss, J. Greiner, M. Ohno, T. Ohsugi, N. Omodei, M. Orienti, E. Orlando, J. F. Ormes, D. Paneque, J. S. Perkins, M. Pesce-Rollins, et al. The imprint of the extragalactic background light in the gamma-ray spectra of blazars. *Science*, 338:1190–, 2012.
- [13] H.E.S.S. Collaboration, A. Abramowski, F. Acero, F. Aharonian, A. G. Akhperjanian, G. Anton, S. Balenderan, A. Balzer, A. Barnacka, Y. Becherini, J. Becker Tjus, K. Bernlhr, E. Birsin, J. Biteau, A. Bochow, C. Boisson, J. Bolmont, P. Bordas, J. Brucker, F. Brun, P. Brun, T. Bulik, S. Carrigan, S. Casanova, M. Cerruti, P. M. Chadwick, A. Charbonnier, R. C. G. Chaves, A. Cheesebrough, G. Cologna, J. Conrad, C. Couturier, M. Dalton, M. K. Daniel, I. D. Davids, B. Degrang, C. Deil, P. deWilt, H. J. Dickinson, A. Djannati-Ata, W. Domainko, L. O’C. Drury, G. Dubus, K. Dutson, J. Dyks, M. Dyrda, K. Egberts, P. Eger, P. Espigat, L. Fallon, C. Farnier, S. Fegan, F. Feinstein, M. V. Fernandes, D. Fernandez, A. Fiasson, G. Fontaine, A. Frster, M. Fling, M. Gajdus, Y. A. Gallant, T. Garrigoux, H. Gast, B. Giebels, J. F. Glicenstein, B. Glck, D. Gring, M.-H. Grondin, S. Hffner, J. D. Hague, J. Hahn, D. Hampf, J. Harris, S. Heinz, G. Heinzlmann, G. Henri, G. Hermann, A. Hillert, J. A. Hinton, W. Hofmann, P. Hofverberg, M. Holler, D. Horns, A. Jacholkowska, C. Jahn, M. Jamroz, I. Jung, M. A. Kastendieck, K. Katarzyski, U. Katz, S. Kaufmann, B. Khelifi, D. Klockhov, W. Kluniak, T. Kneiske, Nu. Komin, K. Kosack, R. Kossakowski, F. Krayzel, H. Laffon, et al. Measurement of the extragalactic background light imprint on the spectra of the brightest blazars observed with h.e.s.s. *Astronomy and Astrophysics*, 550, 2013.
- [14] Alessandro de Angelis, Giorgio Galanti, and Marco Roncadelli. Relevance of axionlike particles for very-high-energy astrophysics. *Physical Review D*, 84:105030, 2011.
- [15] Denis Wouters and Pierre Brun. Irregularity in gamma ray source spectra as a signature of axionlike particles. *Physical Review D*, 86:43005, 2012.
- [16] Pierre Brun. Axion-like particles: possible hints and constraints from the high-energy universe. *Journal of Physics Conference Series*, 460:2015, 2013.
- [17] J. Biteau and D. A. Williams. The extragalactic background light, the hubble constant, and

anomalies: Conclusions from 20 years of tev gamma-ray observations. *The Astrophysical Journal*, 812, 2015.

- [18] Melanie Simet, Dan Hooper, and Pasquale D. Serpico. Milky way as a kiloparsec-scale axionscope. *Physical Review D*, 77:63001, 2008.
- [19] Clare Burrage, Anne-Christine Davis, and Douglas J. Shaw. Active galactic nuclei shed light on axionlike particles. *Physical Review Letters*, 102:201101, 2009.
- [20] Alessandro Mirizzi and Daniele Montanino. Stochastic conversions of tev photons into axion-like particles in extragalactic magnetic fields. *Journal of Cosmology and Astro-Particle Physics*, 12:004, 2009.
- [21] M. Fairbairn, T. Rashba, and S. Troitsky. Photon-axion mixing and ultra-high energy cosmic rays from bl lac type objects: Shining light through the universe. *Physical Review D*, 84:125019, 2011.
- [22] Dieter Horns, Luca Maccione, Manuel Meyer, Alessandro Mirizzi, Daniele Montanino, and Marco Roncadelli. Hardening of tev gamma spectrum of active galactic nuclei in galaxy clusters by conversions of photons into axionlike particles. *Physical Review D*, 86:75024, 2012.
- [23] A. Abramowski, F. Acero, F. Aharonian, F. Ait Benkhali, A. G. Akhperjanian, E. Angner, G. Anton, S. Balenderan, A. Balzer, A. Barnacka, Y. Becherini, J. Becker Tjus, K. Bernl?hr, E. Birsin, E. Bissaldi, J. Biteau, C. Boisson, J. Bolmont, P. Bordas, J. Brucker, F. Brun, P. Brun, T. Bulik, S. Carrigan, S. Casanova, M. Cerruti, P. M. Chadwick, R. Chalme-Calvet, R. C. G. Chaves, A. Cheesebrough, M. Chrtien, S. Colafrancesco, G. Cologna, J. Conrad, C. Couturier, M. Dalton, M. K. Daniel, I. D. Davids, B. Degrange, C. Deil, P. deWilt, H. J. Dickinson, A. Djannati-Ata?, W. Domainko, L. O.'C. Drury, G. Dubus, K. Dutton, J. Dyks, M. Dyrda, T. Edwards, K. Egberts, P. Eger, P. Espigat, C. Farnier, S. Fegan, F. Feinstein, M. V. Fernandes, D. Fernandez, A. Fiasson, G. Fontaine, A. F?rster, M. F?ling, M. Gajdus, Y. A. Gallant, T. Garrigoux, H. Gast, B. Giebels, J. F. Glicenstein, D. G?ring, M.-H. Grondin, M. Grudziska, S. H?ffner, J. D. Hague, J. Hahn, J. Harris, G. Heinzelmann, G. Henri, G. Hermann, O. Hervet, A. Hillert, J. A. Hinton, W. Hofmann, P. Hofverberg, M. Holler, D. Horns, A. Jacholkowska, C. Jahn, M. Jamroz, M. Janiak, F. Jankowsky, I. Jung, M. A. Kastendieck, K. Katarzyski, U. Katz, S. Kaufmann, B. Khlifi, M. Kieffer, S. Klepser, D. Klockov, W. Klu?niak, et al. Constraints on axionlike particles with h.e.s.s. from the irregularity of the pks 2155-304 energy spectrum. *Physical Review D*, 88, 2013.
- [24] Manuel Meyer, Daniele Montanino, and Jan Conrad. On detecting oscillations of gamma rays into axion-like particles in turbulent and coherent magnetic fields. *Journal of Cosmology and Astro-Particle Physics*, 09, 2014.
- [25] Denis Wouters and Pierre Brun. Anisotropy test of the axion-like particle universe opacity effect: a case for the cherenkov telescope array. *Journal of Cosmology and Astro-Particle Physics*, 01, 2014.
- [26] Giorgio Galanti, Marco Roncadelli, Alessandro De Angelis, and Giovanni F. Bignami. Advantages of axion-like particles for the description of very-high-energy blazar spectra, March 1, 2015 2015. 33 pages, 9 figures, additional material added.
- [27] Esra Bulbul, Maxim Markevitch, Adam Foster, Randall K. Smith, Michael Loewenstein, and Scott W. Randall. Detection of an unidentified emission line in the stacked x-ray spectrum of galaxy clusters. *The Astrophysical Journal*, 789, 2014.
- [28] A. Boyarsky, O. Ruchayskiy, D. Iakubovskiy, and J. Franse. Unidentified line in x-ray spectra of the andromeda galaxy and perseus galaxy cluster. *Physical Review Letters*, 113, 2014.
- [29] Tetsutaro Higaki, Kwang Sik Jeong, and Fuminobu Takahashi. The 7 kev axion dark matter and the x-ray line signal. *Physics Letters B*, 733:25–31, 2014.



- [30] Joerg Jaeckel, Javier Redondo, and Andreas Ringwald. 3.55 keV hint for decaying axionlike particle dark matter. *Physical Review D*, 89, 2014.
- [31] Michele Cicoli, Joseph P. Conlon, M. C. David Marsh, and Markus Rummel. 3.55 keV photon line and its morphology from a 3.55 keV axionlike particle line. *Physical Review D*, 90, 2014.
- [32] Kevo N. Abazajian. Resonantly produced 7 keV sterile neutrino dark matter models and the properties of milky way satellites. *Physical Review Letters*, 112, 2014.
- [33] Joseph P. Conlon and Francesca V. Day. 3.55 keV photon lines from axion to photon conversion in the milky way and m31. *Journal of Cosmology and Astro-Particle Physics*, 11, 2014.
- [34] P. A. R. Ade, K. Arnold, M. Atlas, C. Baccigalupi, D. Barron, D. Boettger, J. Borrill, S. Chapman, Y. Chinone, A. Cukierman, M. Dobbs, A. Ducout, R. Dunner, T. Elleflot, J. Errard, G. Fabbian, S. Feeney, C. Feng, A. Gilbert, N. Goeckner-Wald, J. Groh, G. Hall, N. W. Halverson, M. Hasegawa, K. Hattori, M. Hazumi, C. Hill, W. L. Holzapfel, Y. Hori, L. Howe, Y. Inoue, G. C. Jaehnig, A. H. Jaffe, O. Jeong, N. Katayama, J. P. Kaufman, B. Keating, Z. Kermish, R. Keskitalo, T. Kisner, A. Kusaka, M. Le Jeune, A. T. Lee, E. M. Leitch, D. Leon, Y. Li, E. Linder, L. Lowry, F. Matsuda, T. Matsumura, N. Miller, J. Montgomery, M. J. Myers, M. Navaroli, H. Nishino, T. Okamura, H. Paar, J. Peloton, L. Pogosian, D. Poletti, G. Puglisi, C. Raum, G. Rebeiz, C. L. Reichardt, P. L. Richards, C. Ross, K. M. Rotermund, D. E. Schenck, B. D. Sherwin, M. Shimon, I. Shirley, P. Siritanasak, G. Smecher, N. Stebor, B. Steinbach, A. Suzuki, J.-i. Suzuki, O. Tajima, S. Takakura, A. Tikhomirov, T. Tomaru, N. Whitehorn, B. Wilson, A. Yadav, A. Zahn, O. Zahn, and Polarbear Collaboration. POLARBEAR constraints on cosmic birefringence and primordial magnetic fields. *Physical Review D*, 92(12):123509, December 2015.
- [35] D. Grasso and H. R. Rubinstein. Magnetic fields in the early Universe. *Physics Reports*, 348:163–266, July 2001.
- [36] Y. Grossman, S. Roy, and J. Zupan. Effects of initial axion production and photon-axion oscillation on type Ia supernova dimming [rapid communication]. *Physics Letters B*, 543:23–28, 2002.
- [37] Dong Lai and Jeremy Heyl. Probing axions with radiation from magnetic stars. *Physical Review D*, 74:123003, 2006.
- [38] T. K. Kuo and James Pantaleone. Neutrino oscillations in matter. *Reviews of Modern Physics*, 61:937–980, 1989.